Neutron yield studies in JET H-modes

H. Weisen[1], Hyun-Tae Kim[2], J. Strachan[3], S. Scott[3], Y. Baranov[2], J. Buchanan[2], M. Fitzgerald[2], D. Keeling[2], D.B. King[2], L. Giacomelli[4], T. Koskela[5], M.J. Weisen[6], C. Giroud[2], W.G. Core[2], K.-D. Zastrow[2], D.B Syme[2], S. Popovichev[2], S. Conroy[7], I. Lengar[8], L. Snoy[8], P. Batistoni[9], M. Santala[5] and JET contributors*

Eurofusion Consortium JET, Culham Science Centre, Abingdon, OX14 3DB, UK
[1]SPC, Ecole Polytechnique Fédérale de Lausanne, Switzerland,
[2]Culham Centre for Fusion Energy, Abingdon, [3]PPPL, Princeton University, USA,
[4]IFP-CNR, Milano, Italy,
[5]Aalto University School of Science, Espoo, Finland,
[6]University of Strathclyde, Glasgow, UK
[7]EURATOM-VR Fusion Association, Uppsala University, SE-75120 Uppsala, Sweden
[8]EURATOM-MHEST Slovenian Fusion Association, Ljubljana, Slovenija
[9]ENEA, Via E. Fermi, 45, 00044 Frascati, Rome, Italy

**See the author list of "Overview of the JET results in support to ITER" by X. Litaudon et al. to be published in Nuclear Fusion Special issue: overview and summary reports from the 26th Fusion Energy Conference (Kyoto, Japan, 17-22 October 2016)*

Abstract. The measured D-D neutron rate of NBI heated JET baseline and hybrid H-modes in Deuterium is found to be between approximately 50% and 100% of the neutron rate expected from the TRANSP code, depending on plasma parameters. A number of candidate explanations, such as fuel dilution, errors in beam penetration and effectively available beam power have been excluded. As the neutron rate in JET is dominated by beam-plasma interactions, the 'neutron deficit' may be caused by a yet unidentified form of fast particle redistribution. Modelling, which assumes fast particle transport to be responsible for the deficit, indicates that such redistribution would have to happen at time scales faster than the slowing down time and the energy confinement time. Sawteeth and ELMs are found to make no significant contribution to the deficit. There is also no obvious correlation with MHD activity measured using magnetic probes at the tokamak vessel walls. Modelling of fast particle orbits in the 3D fields of NTM's shows that realistically sized islands can contribute only a few % to the deficit.

1. INTRODUCTION

We refer as «neutron deficit» to a situation where the measured neutron rate falls short of expectations based on ion orbit codes such as TRANSP/NUBEAM [1], assuming only

collisional fast ion orbit diffusion. The neutron deficit affects discharges in JET-C and in JET-ILW discharges and ranges from 0 to 50% typically. Frustratingly, despite being well characterised by the study here presented, the neutron deficit has so far eluded all attempts at identifying its causes. In JET, unlike ITER, neutrons are primarily from beam-thermal reactions and the causes of the neutron deficit are believed to due to processes affecting the fast ion-thermal reactivity, such as fuel dilution, NBI deposition and fast ion transport. Previous studies of the neutron deficit in JET have focussed on the trace Tritium campaign in 2003 [2,3]. The study presented here is based on Deuterium discharges, mostly from the JET carbon phase under EFDA (JET-C, 2001-2009) and cover a wide range of plasma conditions in baseline H-mode, hybrid scenarios. The data used are from a database (JETPEAK) previously used for particle and momentum transport studies [4], augmented by the wide range of variables required for the present study. Data were averaged over sampling windows of typically 0.5-1 second duration in stationary conditions. A subset of 317 samples for which TRANSP calculations were produced is presented here and covers the following ranges:

$0.8\text{MA} \le I_p \le 4\text{MA}$, $1\text{T} \le B_T \le 3.4\text{T}$, $2\ \text{MW} < P_{NBI} < 23\text{MW}$, $2.1 \le q_{95} \le 4.7$, $0.47 \le H98 \le 1.4$

$1.5\times10^{19} \le \langle n_e \rangle \le 9.4\times10^{19}\text{m}^{-3}$, $0.002 \le \langle n_C \rangle / \langle n_e \rangle \le 0.06$, $1.4 \le Z_{eff}(\text{VB}) \le 4$, $0.06 \le \tau_E \le 0.5\text{s}$,

Here n_C refers to the carbon density from CXRS, the brackets refer to volume averages, Z_{eff}(VB) is the effective charge as measured by visible bremstrahlung, τ_E is the energy confinement time based on the kinetic stored energy calculated from the plasma profiles and H98 is τ_E normalised to the IPB98(y,2) scaling. Discharges with $P_{ICRH}/P_{NBI}>0.1$, increased toroidal ripple, 3D fields from internal coils and the entire trace T campaign were excluded. Neutron rates were measured using the JET fission chambers, as recently retroactively recalibrated [5].

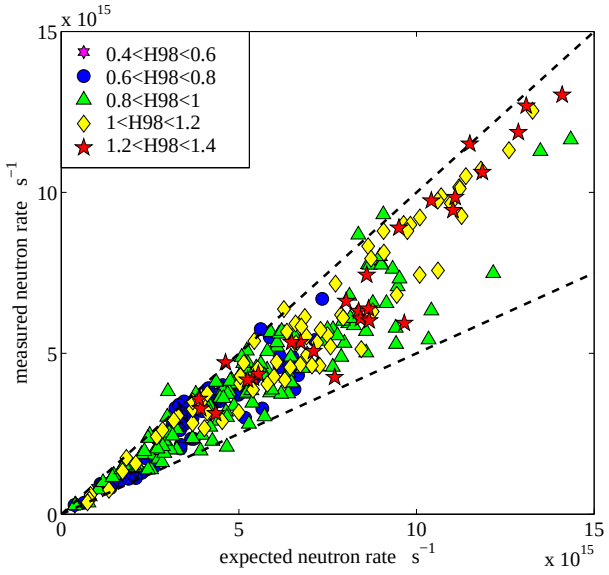

Fig.1 Measured v expected neutron rates in JET-C

TRANSP simulations for the 317 samples from JET-C were produced using T_i, the toroidal rotation ω_ϕ and the dilution inferred from the carbon density n_C measured using CXRS and electron density and temperature from LIDAR Thomson scattering. Importantly, no ad-

hoc adjustments to the measurements were made prior to the TRANSP calculations with the purpose of improving agreement between calculations and measurements. The measured neutron rates are in the range 50-100% of the total neutron rate expected from TRANSP, as seen in fig.1. The symbols refer to classes of H98, showing that the neutron deficit affects the entire JET operating domain and spans the range 50-100% largely irrespectively of confinement quality.

Fig.2 shows that the neutron deficit also affects JET-ILW (i.e. after JET was equipped with Tungsten and Be PFC's) plasmas by comparing pairs of similar baseline H-modes in JET-C and JET-ILW with matching I_p=2.5MA, B_T=2.7T, $\langle n_e \rangle$ and P_{NBI} (in the range 14-17MW) and triangularity, as detailed in [6]. Their main differences were lower temperatures in the JET-ILW cases and additional Nitrogen impurity injection in 7 out of the 10 cases. The values of Zeff in these discharges with N injections were comparable to those in JET-C, while the ones without N injection were significantly lower. CXRS ion temperature measurements were not available for the JET-ILW discharges, however they were chosen to have high enough density ($7\times10^{19}m^{-3}<\langle n_e \rangle <10^{20}m^{-3}$) to safely allow the assumption $T_i=T_e$ in the TRANSP calculations. The JET-ILW discharges had a clearly lower confinement (H98≈0.63 on average) than the JET-C cases (H98≈0.9). The deficit was also somewhat larger, with the ratio of measured to expected neutrons rates, $R^*_N=R_N/R_{NTRANSP}$ ≈0.7 for the 10 JET-C samples and R^*_N ≈0.64 on average for the 10 JET-ILW samples, irrespective of whether Nitrogen was injected. As in the JET-C case, for high temperature discharges such as hybrid scenarios, R^*_N is closer to 1, although uncertainties on Ti are larger in JET-ILW than they were in JET-C.

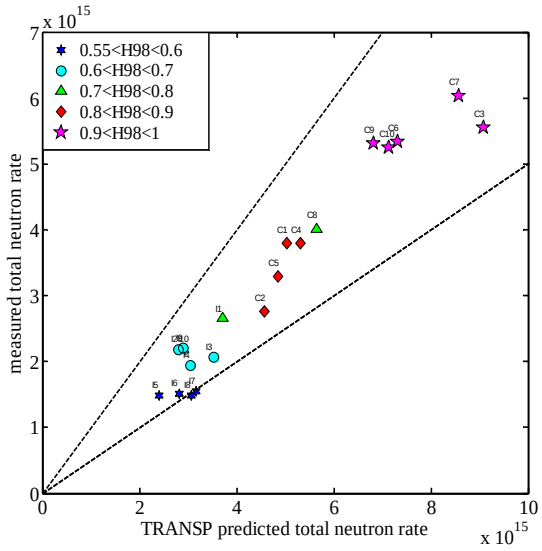

Fig.2 Measured versus expected neutron rates for 10 pairs of discharges with members from JET-C (labelled C1-C10) and JET-ILW (labelled I1-I10). I1,I2 and I3 were nitrogen seeded with Z_{eff} not exceeding that of their JET-C counterparts.

Table 1 shows a correlation matrix (in %) between the ratio of the measured neutron rates and the ones expected from TRANSP and several plasma parameters for the JET-C dataset. As is typical for data representative of the entire operating domain, there are strong correlations

between parameters. The top line has the correlation coefficients of R^*_N with the parameter set and the second has those for beam plasma interactions only, as inferred by subtracting the calculated thermal and beam-beam reactions. The full list of variables in the table is given in the legend of the table.

	RNT/TRANSP	B-P/TRANSP	ZEFF VB	C_C 33	NEAV	IP	PNBI	H98	ω max	TE33	TE33/66	Ti/Te 33	β_N	β fast	Tslo/τE	MHD1/IP	MHD2/IP
RNT/TRANSP		95		13	-10		25	21	45	34	15	30	30	12	11	24	
B-P/TRANSP	95				-20	-20	11	14	28	16	24	16	25	12	14	21	
ZEFF VB					-28					58	27	11		13	32	-15	
C_C 33	13																
NEAV	-10	-20	-28			54	28		-21		-33	-22	28	-52	-74	14	-18
IP		-20			54		16	-39	-17	26	-17	-17	-29	-53	-49		-32
PNBI	25	11			28	16		29	48	21	-19	25	46	39	10	19	22
H98	21	14				-39	29		60		-32	39	85	63		41	37
ω max	45	28			-21	-17	48	60		32	-11	48	50	52	20	16	20
TE33	34	16	58			26	21		32		32		16	19	29		-10
TE33/66	15	24	27		-33	-17	-19	-32	-11	32		-15	-27		35	-18	-18
Ti/Te 33	30	16	11		-22	-17	25	39	48		-15		38	43	22	22	30
β_N	30	25			28	-29	46	85	50	16	-27	38		72	13	50	55
β fast	12	12	13		-52	-53	39	63	52	19		43	72		61	29	61
Tslo/τE	11	14	32		-74	-49	10		20	29	35	22	13	61			28
MHD1/IP	24	21	-15		14		19	41	16		-18	22	50	29			29
MHD2/IP					-18	-32	22	37	20	-10	-18	30	55	61	28	29	

TABLE 1. Matrix of correlation coefficients in % of measured/predicted neutron rates and a selection of plasma parameters. Matrix elements with correlation coefficients below 10% are insignificant and are blanked.
1) RN/TRANSP ratio of measured to TRANSP predicted total neutron rate
2) B-P/TRANSP=$(R_{Nmeas}-R_{Nth}-R_{Nbb})/R_{Nbp}$
3) ZeffVB Zeff from visible bremstrahlung
4) C_c33 carbon concentration from CXRS at ρ=0.33
5) NEAV line average electron density
6) IP plasma current
7) PNBI neutral beam power
8) H98 confinement enhancement over IPB98,y9) Ti33 ion temperature at ρ=0.33
10) ω33 ion toroidal rotation at ρ=0.33
11) Te33 electron temperature at ρ=0.33
12) TiTe33 temperature ratio at ρ=0.33
13) β_N normalised plasma beta
14) β_{fast} NBI fast ion beta
15) T_{slow}/τ_E ration of NBI ion slowing down time at ρ=0.33 to energy confinement time
16-17) Amplitude of N=1 & N=2 MHD activity from external probes, normalised to I_P

Negative values indicate anti-correlations. As can be seen from the table, R^*_N correlates with measured plasma parameters, being largest in discharges with high T_e, T_i, β_N, ω_ϕ such as hybrid scenarios. Simple linear regressions of R^*_N, as shown in fig.3, using a small number (3-4) of plasma parameters achieve standard deviations near 10%, well within the best expectation, given that the key parameters governing the neutron rate (e.g. T_e, T_i, P_{NBI}, n_e, n_C) are quoted with errors of the order of 10%. They suggest that the neutron deficit may in part

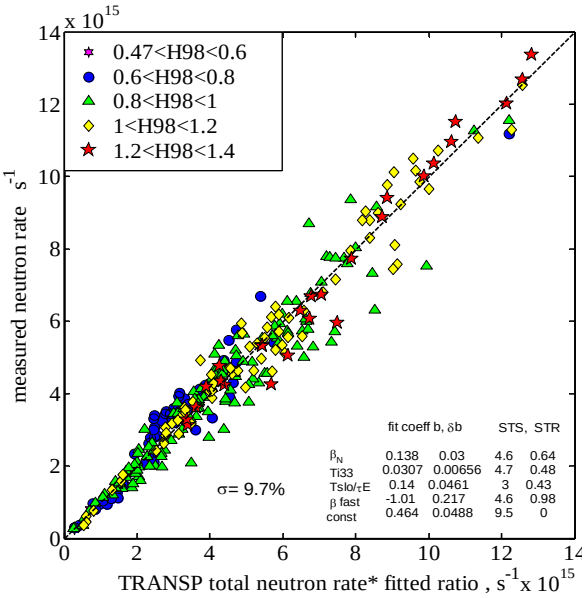

Fig.3 Measured neutron rate versus TRANSP prediction corrected with a regression. STS is the statistical significance for a 90% confidence interval and STR is the normalised statistical relevance.

be a matter of plasma physics, but do not exclude the possibility that systematic experimental errors may also play a role. The parameters in the example regression are β_N, $T_i(\rho=1/3)$, $T_{slow}(\rho=1/3)/\tau_E$ and $\beta_{fast}= W_{fast}/(B^2/2\mu_0)$. The latter has a negative coefficient, perhaps indicating that fast ion pressure driven modes may play a role. $T_{slow}(\rho=1/3)$ is the fast ion slowing down time from the birth energy to thermal evaluated at 1/3 of the minor radius. These parameters should not be interpreted as being causally related to the deficit.

2. POSSIBLE CAUSES OF THE NEUTRON DEFICIT

2.1. Dilution by light impurities

The most often heard hypothesis is that dilution by light impurities (Carbon in JET-C and Beryllium in JET-ILW) are more substantial than inferred from the measurements, resulting in Deuterium ion densities that are lower than expected. However neither Zeff, nor the core carbon density measured using CXRS correlate with the neutron deficit. The fact that JET-ILW plasmas, which have significantly lower dilution than JET-C plasmas, but have a worse deficit, is also at odds with an explanation based on dilution.

2.2. Overestimate of NBI power

A recent study of the overall energy balance in JET, as measured from the energy losses (conduction to PFC's, radiation) and inputs shows that ~25% of the input power are unaccounted for [7], suggesting among other explanations that the actual NBI power may fall short of the expected NBI power, which might explain both the power balance and the neutron deficits. A neutral beam power mis-calibration appears to have been at the origin of discrepant TRANSP predictions and neutron rate measurements in DIII-D [8]. However, a careful review of the uncertainties of the JET NBI power measurements concluded that the uncertainty in the NBI power is 9%, of which 5.9% are due to uncertainties in the beam transmission and 3% in the neutralisation efficiency. The parameter dependences of R^*_N are

also hard to explain in terms of variations of the NBI power. This is shown by introducing R^*_N as an additional variable in a confinement scaling regression containing the usual regression variables, such as I_p, B_T, n_e and P_{NBI}. If R^*_N were a measure of the ratio of the real to the expected NBI power, then R^*_N should be a significant contributor to the scaling, with an exponent equal to that of P_{NBI}. We find that regressions including R^*_N do provide scalings akin to IPB98(y,2), but the exponent for R^*_N is statistically insignificant and irrelevant (zero within errors), i.e. low R^*_N is not indicative of NBI underperformance.

2.3. NBI beam penetration overestimated

Another hypothesis is that beam penetration to the core may be lower than expected, resulting in a smaller than expected fast ion population in the core and a larger fraction deposited in the colder periphery, leading to a lower beam-plasma neutron rate. As part of an NBI commissioning procedure, the transmission of one of the NBI beamlets (PINI's) to the inner wall was inferred from the ratio of the deposited power, measured using an IR camera, in the presence and in the absence of a plasma. The measured transmission through the plasma (6.8%) matched the predicted transmission (7.3%), validating the beam deposition calculation. If the beam attenuation was systematically underestimated the error would scale with the average plasma density. However, the plasma density correlates very weakly with the neutron deficit, as seen in table 1. Furthermore, the peakedness of the NBI power deposition profile, expressed as $\langle q_{NB}(\rho<1/3)\rangle/\langle q_{NB}(\rho<1)\rangle$, ranging from 0.4 (hollow) to 5 (very peaked), is uncorrelated with the deficit, confirming that potential errors in the beam stopping calculations do not explain the neutron deficit. The TRANSP calculations were done with the PREACT [8] code as part of the TRANSP runs. For 28 cases, TRANSP runs using the ADAS [10] atomic data were additionally performed for comparison. The neutron rates predicted by the two models agree within 2% for 24 of the cases and within 4% for the 4 remaining ones. To conclude, there is no evidence for the beam deposition calculations to be at fault.

2.4 Transport by broadband turbulence

Drift wave type turbulence, such as electrostatic ITG turbulence is largely believed to be the main contributor to heat transport in tokamaks, prompting the question whether turbulence may also cause fast ion transport, carrying NBI ions to colder parts of the plasma or even leading to their loss. A simple model was used for assessing a hypothetical relation between fast ion and thermal energy transport. It calculates the radial diffusion of fast ions, assuming $D_f \propto \chi_i$, together with the fast ion slowing down and associated neutron production. Neutron rates are reduced by transport because of the increased (unproductive) slowing down on the electrons at the lower T_e experienced by fast ions having moved outwards, as well as due to the reduced $\langle\sigma v\rangle_{DD}$ at lower T_i. Fig.4 shows R^*_N versus the ratio obtained from assuming

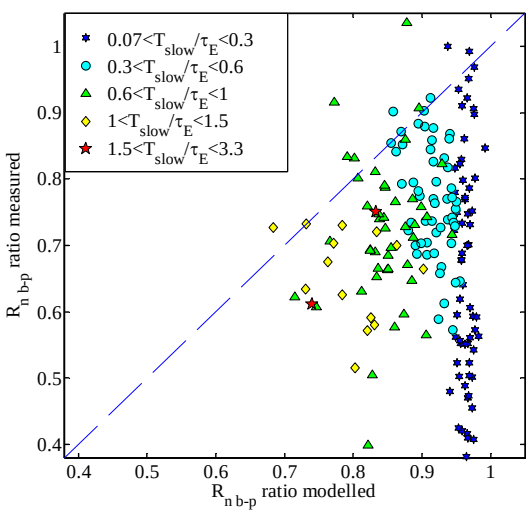

Fig.4 Measured versus modelled beam-thermal R^*_N, assuming $D_f=\chi_i$ and $D_f=0$

$D_f=\chi_i$ from the power balance and $D_f=0$ using the model. It is plain that the observed dependencies are not reproduced by the model. In particular, ions with $T_{slow}(\rho=1/3)/\tau_E<0.3$ (blue stars) should be immune to transport at the time scale of τ_E, but the results show to the contrary, that this class of data spans the whole range, from no deficit to the worst. This result, together with the above mentioned absence of any relation of R^*_N with energy confinement makes it unlikely that there is a significant relationship between heat and fast ion transport.

2.5. Sawteeth, ELMs and NTMs

Fast ion redistribution by a variety of MHD modes, such as sawteeth, NTMs and fishbones, provides a potential explanation. Neutron rates in most baseline H-modes are too low for measuring sawteeth using the JET neutron camera. This drawback has been overcome by the boxcar-ing of 2600 quasi-identical sawteeth with 0.5ms time resolution from 132 repeated pulses, using a central ECE signal for crash timing. The result shows that neutron sawteeth (reflecting those of the underlying fast ions) are very similar to those of other plasma parameters such as T_e, with a ~16% crash for the central channel and inverted neutron sawteeth outside the inversion radius. Ad-hoc modelling of the mixing, as well as the (selectable) sawtooth model in TRANSP, show that mixing by sawteeth can account at best for a few % of the neutron deficit on a sawtooth cycle averaged basis, when sawteeth are present at all. Boxcar-ing of 18000 ELMs has revealed no discernible effect of the ELMs on the neutron rates. An analysis of MHD activity based on the JET high resolution toroidal array and spanning the mode number range $-10<N<10$ has so far revealed no significant correlation between mode activity and the neutron deficit. It is tempting to see this as supportive of 3D ASCOT Monte Carlo orbit simulations of fast NBI ions in the 3D fields of NTM's, which show that NTM's can only account for a modest reduction in neutron rates [11]. Fig.5 (left) shows the fast ion density profiles for a series of ASCOT calculations for a plasma with a 25% neutron deficit and having an m/n=3/2, 10cm wide island at mid-radius. Simulations were produced for island widths ranging from 0 (no island) to 25 cm. While there is a clear reduction of the core fast ion density, the impact on the total neutron rate remains modest (10%) even for the largest 25 cm wide modelled island (fig.5 right), which is much larger than typically observed in JET. The simulations were repeated with strings of partially

overlapping 3/2, 2/1, 3/1 islands causing extensive stochastisation connecting the core to the LCFS. Even in this very unrealistic case, a neutron deficit of 13-18% percent remained, depending on whether the islands were assumed to be stationary or rotating with the plasma.

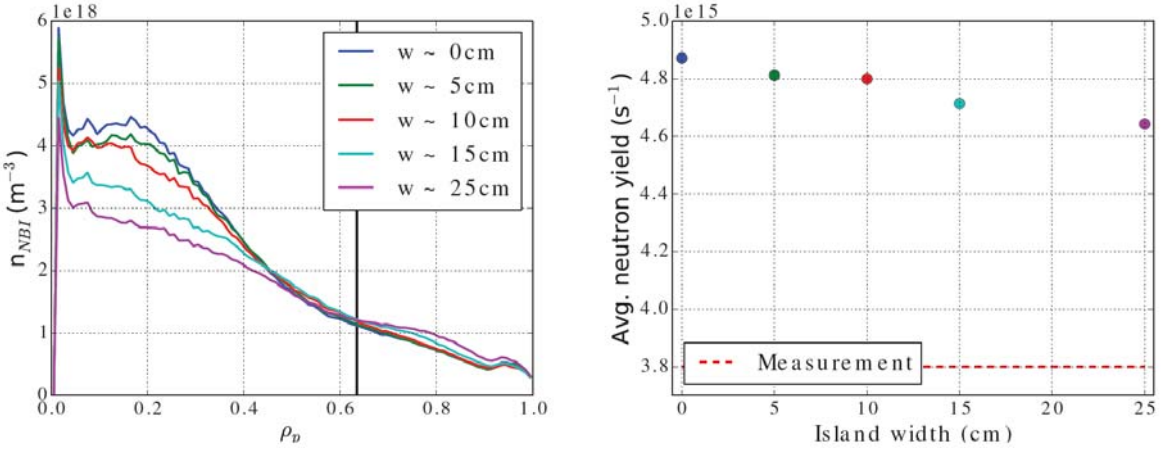

Fig. 5 Left: ASCOT calculations of fast ion profiles for different island widths
Right: Neutron rates versus island widths

3. CONCLUSIONS

An examination of popular candidates for explaining the neutron deficit in JET (dilution, NBI power and penetration, transport by the same channels as thermal transport and transport by MHD) has led to the conclusion that these mechanisms can contribute only modestly (a few %) to the deficit or have parameter dependencies which are inconsistent with observations. This doesn't rule out that some still to be identified form of fast ion transport may be causing the deficit, however it also suggests that possible explanations not related to plasma physics processes should get more attention.

4. References

[1] A. Pankin et al, Computer Phys. Comm. **159**, No. 3, (2004) 157
[2] Y. Baranov et al, PPCF **51** (2009) 044004
[3] M. Nocente et al, Nucl. Fusion **54** (2014) 104010
[4] H. Weisen et al, Nucl. Fusion **52** (2012) 114024
[5] D.B. Syme, S. Popovichev, S. Conroy et al, Fusion Engineering and Design, **89** (2016), 2766
[6] Hyun-Tae Kim et al, PPCF **57**, 2015 065002
see also Hyun-Tae Kim et al, FEC26, Kyoto 2016 (this conf.), TH/P-17
[7] G. Matthews et al, PSI, 2016
[8] W.W. Heidbrink et al, Nucl. Fusion 52 (2012) 094005
[9] C.F. Barnett et al, Atomic Data for Fusion, **1**, ORNL-6086/V1 (July 1990)
[10] http://www.adas.ac.uk/
[11] T. Koskela et al, 42nd EPS, 2015, P2.106

Acknowledgement: This work was carried out within the framework of the EUROfusion Consortium and received funding from the EURATOM research and training programme 2014-2018 under grant agreement No 633053. The views and opinions expressed herein do not necessarily reflect those of the European Commission.